

This article was downloaded by: [Tomsk State University of Control Systems and Radio]

On: 20 February 2013, At: 11:48

Publisher: Taylor & Francis

Informa Ltd Registered in England and Wales Registered Number: 1072954

Registered office: Mortimer House, 37-41 Mortimer Street, London W1T 3JH, UK



## Molecular Crystals and Liquid Crystals

Publication details, including instructions for authors and subscription information:

<http://www.tandfonline.com/loi/gmcl16>

### Calorimetric Investigations of the Liquid Crystalline Material Heptyloxybenzylidene-Heptylaniline (70.7)

J. Thoen<sup>a</sup> & G. Seynhaeve<sup>a</sup>

<sup>a</sup> Laboratorium voor Molekulfysika, Katholieke Universiteit Leuven, Celestijnenlaan 200D, B-3030, Leuven, Belgium

Version of record first published: 17 Oct 2011.

To cite this article: J. Thoen & G. Seynhaeve (1985): Calorimetric Investigations of the Liquid Crystalline Material Heptyloxybenzylidene-Heptylaniline (70.7), *Molecular Crystals and Liquid Crystals*, 127:1, 229-256

To link to this article: <http://dx.doi.org/10.1080/00268948508080842>

PLEASE SCROLL DOWN FOR ARTICLE

Full terms and conditions of use: <http://www.tandfonline.com/page/terms-and-conditions>

This article may be used for research, teaching, and private study purposes. Any substantial or systematic reproduction, redistribution, reselling, loan, sub-licensing, systematic supply, or distribution in any form to anyone is expressly forbidden.

The publisher does not give any warranty express or implied or make any representation that the contents will be complete or accurate or up to date. The accuracy of any instructions, formulae, and drug doses should be independently verified with primary sources. The publisher shall not be liable

for any loss, actions, claims, proceedings, demand, or costs or damages whatsoever or howsoever caused arising directly or indirectly in connection with or arising out of the use of this material.

# Calorimetric Investigations of the Liquid Crystalline Material Heptyloxybenzylidene-Heptylaniline (70.7)<sup>†</sup>

J. THOEN and G. SEYNHAEVE

*Laboratorium voor Molekuulfysika, Katholieke Universiteit Leuven, Celestijnenlaan 200D, B-3030 Leuven, Belgium*

*(Received July 19, 1984)*

Using an adiabatic scanning calorimeter we have studied the thermal behavior of the liquid crystalline material heptyloxybenzylidene-heptylaniline in the temperature range between 52°C and 86°C. In this temperature range a rich variety of liquid crystalline and plastic crystalline phases and phase transitions could be studied. The isotropic to nematic (NI) transition and the nematic to smectic A (NA) transition (only 0.3°C below  $T_{NI}$ ) are both first-order with a latent heat of 2.1 ( $\pm 0.1$ ) kJ/mol and 2.2 ( $\pm 0.1$ ) kJ/mol respectively. The first-order nature of the NA transition is in accordance with recent observations for systems with similarly small nematic ranges. The smectic A to smectic C (AC) transition is second-order within the experimental resolution. The observed anomaly in the specific heat  $C_p$  for the AC transition is not consistent with the theoretically expected XY behavior. It can, however, be described rather well with a mean field theory. The transition from the smectic C to the plastic B phase is first-order with a latent heat of 2.9 ( $\pm 0.1$ ) kJ/mol. The transition between the plastic B and G phases is also first-order but with a rather small latent heat of 0.135 ( $\pm 0.015$ ) kJ/mol. In the B phase we have observed several thermal anomalies, which can be associated with different restacking transitions.

## INTRODUCTION

Many liquid crystalline materials exhibit a rich variety of phases intermediate between a normal isotropic liquid and a crystalline solid.<sup>1</sup> Several compounds of the N-(4-n-alkoxybenzylidene)-4-n'-alkylani-

<sup>†</sup>Paper presented at the Tenth International Liquid Crystal Conference, York, G.B., July 15–21, 1984.

line (nO.m) homologous series have a very diverse phase behavior close to room temperature.<sup>2</sup> In particular the complex smectic polymorphic behavior for many of these materials has attracted considerable attention over the last few years.<sup>3-6</sup> Results of high-resolution ac-calorimetry<sup>7-10</sup> and X-ray scattering<sup>9,11-13</sup> investigations of phases and phase transitions for several nO.m compounds have recently been reported.

In this paper we present high-resolution adiabatic scanning calorimetric results for N-(4-n-heptyloxybenzylidene)-4-n'-heptylaniline (7O.7). Besides the fact that no high-resolution calorimetric data were available for 7O.7, this material was chosen because of its rich polymorphism (see Figure 1) and its sufficiently wide smectic C phase with a smectic C to A transition at a convenient temperature. This allows us to study in detail the critical behavior of this supposedly second-order phase transition. Additional motivation was provided by the X-ray study of Collett *et al.* which showed several restacking transitions in the plastic crystalline B phase.<sup>12</sup> No latent heat or thermal anomaly had previously been associated with these restacking transitions.

## EXPERIMENTAL

The measurements have been carried out with the same adiabatic-scanning calorimeter as used previously for measurements on cyanobiphenyl compounds.<sup>14-16</sup> Full details of the calorimeter and its possible modes of operation can be found elsewhere.<sup>17</sup>

In our principal mode of operation of the scanning calorimeter we apply a constant heating power  $P$  to the measuring cell. The temperature versus time curve  $T(t)$  is the principal experimental result. The  $T(t)$  experimental curve directly results in the enthalpy of the sample:<sup>14</sup>

$$H(T) = H(T_s) + P(t - t_s), \quad (1)$$

where the index  $s$  refers to the starting conditions of the run. The heat capacity  $C_p(T)$  can also be derived from the direct  $T(t)$  data by means of the relation

$$C_p = P/\dot{T}. \quad (2)$$

The rate  $\dot{T}$  is obtained via numerical differentiation. With this heat-

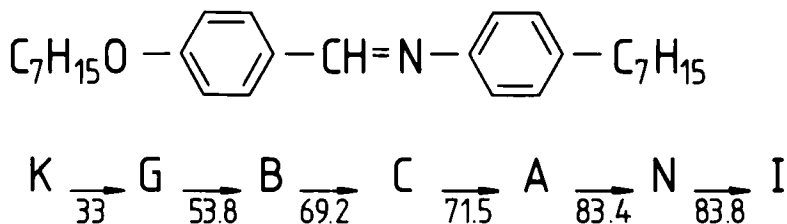


FIGURE 1 Structural formula and phase transition temperatures (in °C) between the different phases of 7O.7 (N-(4-n-heptyloxybenzylidene)-4-n'-heptylaniline): isotropic (I), nematic (N), smectic A (A), smectic C (C), plastic B (B), plastic G (G) and solid crystalline (K).

ing-rate method, it is thus possible to obtain detailed information on the temperature dependence of the heat capacity, and it also allows us to measure the latent heats if present. This is of course an important advantage compared to the ac-calorimetric method, where no latent heats can be measured, and differential scanning calorimetry (DSC), where true latent heats can hardly be distinguished from pretransitional increases of the heat capacity.<sup>18,14</sup>

The (7O.7) material studied was obtained from CPAC-Organix.<sup>19</sup> A sample cell<sup>15</sup> with a maximum volume of 10 cm<sup>3</sup> was filled with 8.05 g (or  $2.025 \times 10^{-2}$  mole) of 7O.7. Measurements have been carried out over the temperature range of 52°C to 86°C, covering, as can be seen in Figure 1, six different phases. Because of the very slow heating rates ( $\approx 0.05$  K/h) and the periodic need for bridge readjustments (because of differences in temperature coefficients of the thermistors) in the servosystems,<sup>17</sup> the indicated temperature interval has been measured in several shorter runs. Some runs with different scanning rates cover the same temperature range (near a phase transition) to test the consistency of the results. In Table I the

TABLE I

Relevant experimental parameters for the heating and cooling runs in 7O.7

Run	T-range (°C)	Transition	$\dot{T}_s$ (K/h)
1	67.19–74.51	BC, CA	0.055
2	71.12–72.22	CA	0.022
3	54.19–67.28		0.078
4	53.08–57.36	GB	0.060
5	57.88–64.62		0.048
6	74.09–79.43		0.051
7	80.50–85.81	AN, NI	0.057
8	55.89–52.22	GB	–0.063
9	52.76–54.66	GB	0.042

relevant experimental parameters for the different runs are summarized. It should be noted that all the runs have been carried out for rather low scanning rates between 0.08 and 0.02 K/h, which is more than three orders of magnitude slower than for DSC measurements.

## RESULTS AND DISCUSSION

In Figure 2 a general overview for the reduced heat capacity per mole  $C_p/R$  (with  $R$  the gas constant) is given for the entire temperature range investigated. Several of the transitions between the different phases show appreciable pretransitional effects. It can also be observed that in the B phase small thermal features are present. The different phases and phase transitions will now be discussed in more detail in order with decreasing temperature.

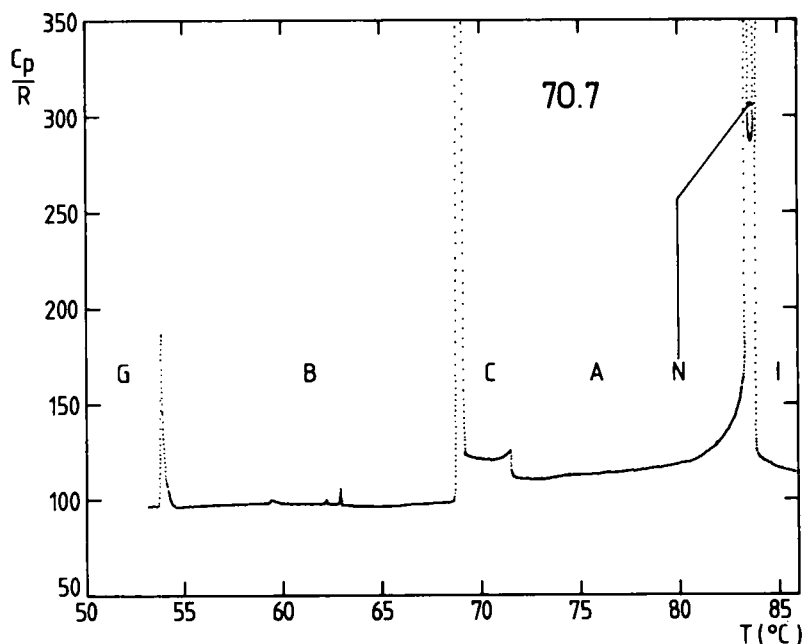


FIGURE 2 General overview for the reduced heat capacity per mole  $C_p/R$  (with  $R$  the gas constant) for the entire temperature range investigated and covering all phases indicated in Figure 1 between the plastic G phase and the isotropic phase.

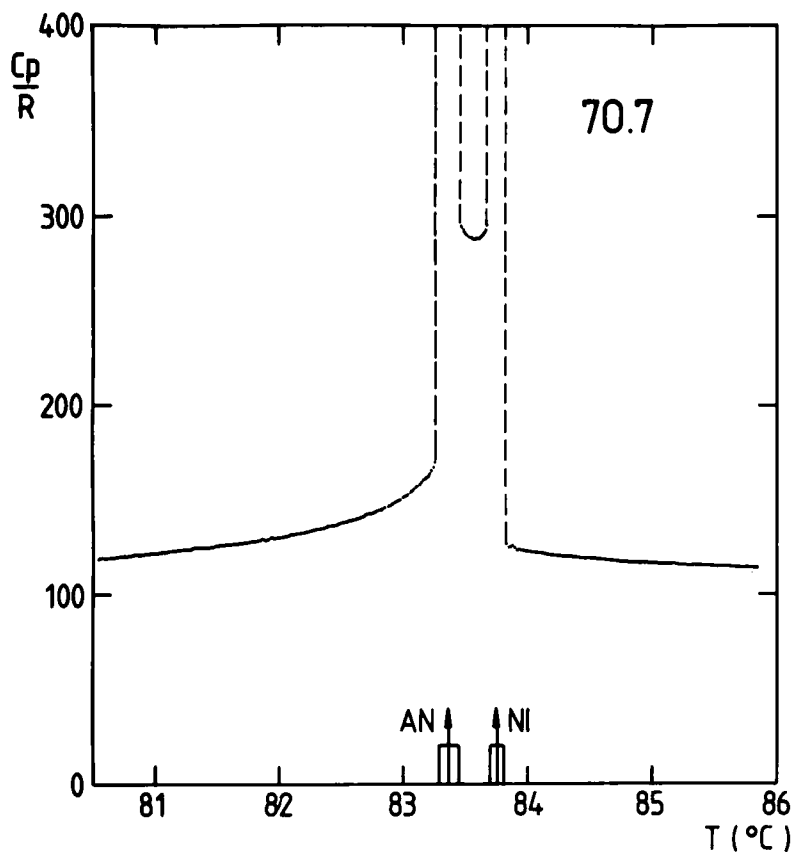


FIGURE 3 Reduced heat capacity per mole for 70.7 near the AN and NI phase transitions. The vertical dashed lines indicate the first-order nature of the transition, and the separation between the lines for the given transition correspond with the two phase region.

### 1. The NI and AN transitions

In Figure 3 a more detailed picture is given for  $C_p/R$  near the NI and AN transitions. Both transitions are first order, which can be clearly seen from Figure 4. The two transitions also show a slight impurity broadening. The widths of the two phase regions are indicated in Figures 3 and 4. For the NI transition there is a  $0.15^\circ\text{C}$  wide two phase region between  $83.83^\circ\text{C}$  and  $83.68^\circ\text{C}$ . For the NA transition we have  $\Delta T_{AN} = 0.21^\circ\text{C}$  between  $83.48^\circ\text{C}$  and  $83.27^\circ\text{C}$ . For the latent heats of the transitions we obtain:  $\Delta H_{NI} = 2.1 (\pm 0.1)$  kJ/mole and

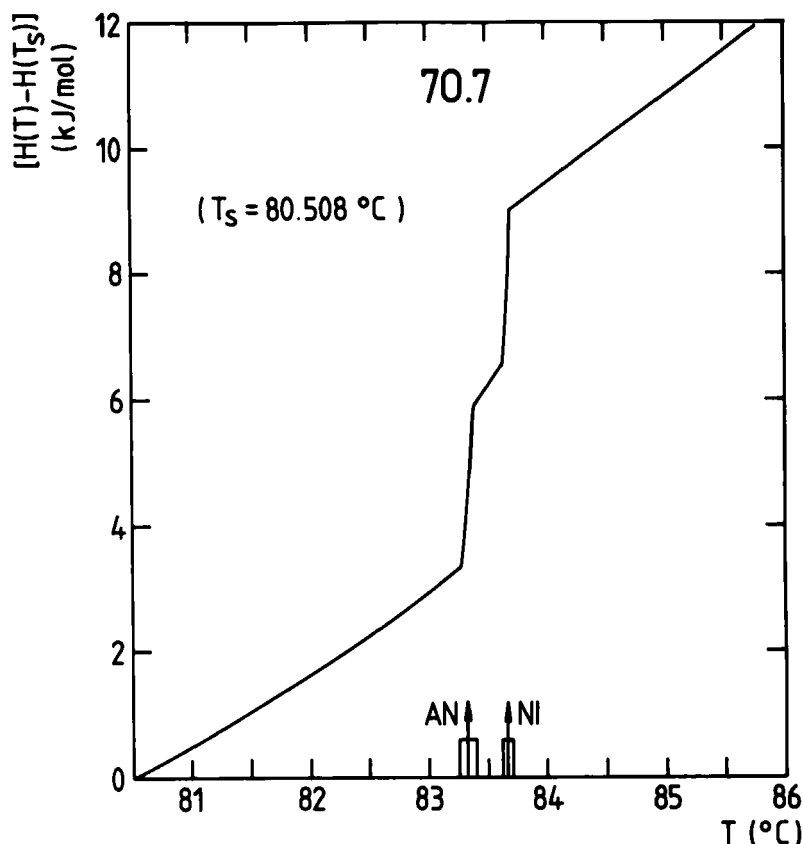


FIGURE 4 Temperature dependence of the enthalpy near the smectic A to nematic (AN) and the nematic to isotropic (NI) phase transitions in 70.7. The width of the two phase region is indicated on the temperature axis.

$\Delta H_{NA} = 2.2 (\pm 0.1)$  kJ/mole. These latent heat values are corrected for the energy ( $\approx 0.3$  kJ/mole) needed to heat the liquid crystal through the two phase region. In the isotropic phase there is only a small pretransitional increase of  $C_p/R = 11$  between  $86^\circ\text{C}$  and  $83.68^\circ\text{C}$ . In the A phase the pretransitional increase is more pronounced:  $\Delta C_p/R = 45$  between  $73^\circ\text{C}$  and  $83.27^\circ\text{C}$ . In the small nematic phase range  $C_p/R$  is about a factor of two larger than in the A or I phases. Apparently this is caused by a combination of AN and NI pretransitional increases.

The fact that we clearly have a first order AN transition deserves some further comments. It has been pointed out by de Gennes<sup>1,20</sup> on



the basis of a Landau expansion of the free energy, that the AN transition can either be second or first order depending on the width of the nematic range. Large and small nematic ranges give second and first order transitions respectively. A tricritical point would occur at the change from first to second order. On the basis of a molecular model McMillan<sup>21</sup> found that the tricritical point should occur for  $T_{AN}/T_{NI} = 0.87$ . This general picture was recently<sup>16,22</sup> verified for mixtures of nonylcyanobiphenyl (9 CB) and decylcyanobiphenyl (10 CB) and also for 9S5, 10S5 and 11S5, compounds of the 4-n-pentyl-phenylthiol-4'-n-alkyloxybenzoate ( $\bar{n}$ S5) homologous series. However, the tricritical  $T_{AN}/T_{NI}$  value was found to be 0.984 ( $\bar{n}$ S5) and 0.994 (nCB) respectively, which is much larger than that predicted by McMillan. Thus first order transitions only occur for very small nematic ranges. This is the case for 7O.7 which has a  $T_{AN}/T_{NI} \approx 0.999$  value, close enough to unity to make the AN transition strongly first order.

## 2. The AC transition

Two different runs have been carried out for the AC transition. The first run (run 1 of Table I) was measured with a scanning rate  $\dot{T}$  of about 0.055 K/h. This run also covered the B to C phase transition, which will be discussed in more detail in the next section. Run 2 of Table I was carried out with a 2.5 times slower scanning rate and covered the temperature range between  $T_{AC} - 0.3^\circ\text{C}$  and  $T_{AC} + 0.6^\circ\text{C}$ . In Figure 5 detailed  $C_p/R$  data from both runs are displayed. From a careful comparison of both runs it was found that  $T_{AC}$  for run 2 was 34 mK below that of run 1. In Figure 5 all data points of run 2 have been shifted up by 34 mK. After this shift in temperature scale for run 2 one can observe very good agreement between the two sets of data.

The  $C_p$  data presented in Figure 5 were calculated with Eq. (2) from the direct  $T(t)$  experimental results of run 1 and run 2. As pointed out above the enthalpy behavior can also be obtained via Eq. (1). In order to define more clearly the anomalous part in the enthalpy we have subtracted a large background  $H_b(T) = \int_{T_s}^T C_p^\infty(T) dT$  from the total  $H(T) - H(T_s)$  results of run 1, see Figure 6. The  $C_p^\infty(T)$  behaviour, which is indicated in Figures 7 and 8, was obtained from a fit with a mean field model (see below).

In Figure 6 there is no indication for a first order discontinuity in the enthalpy at  $T_{AC}$ . From the data of run 1 in Figure 6 and from

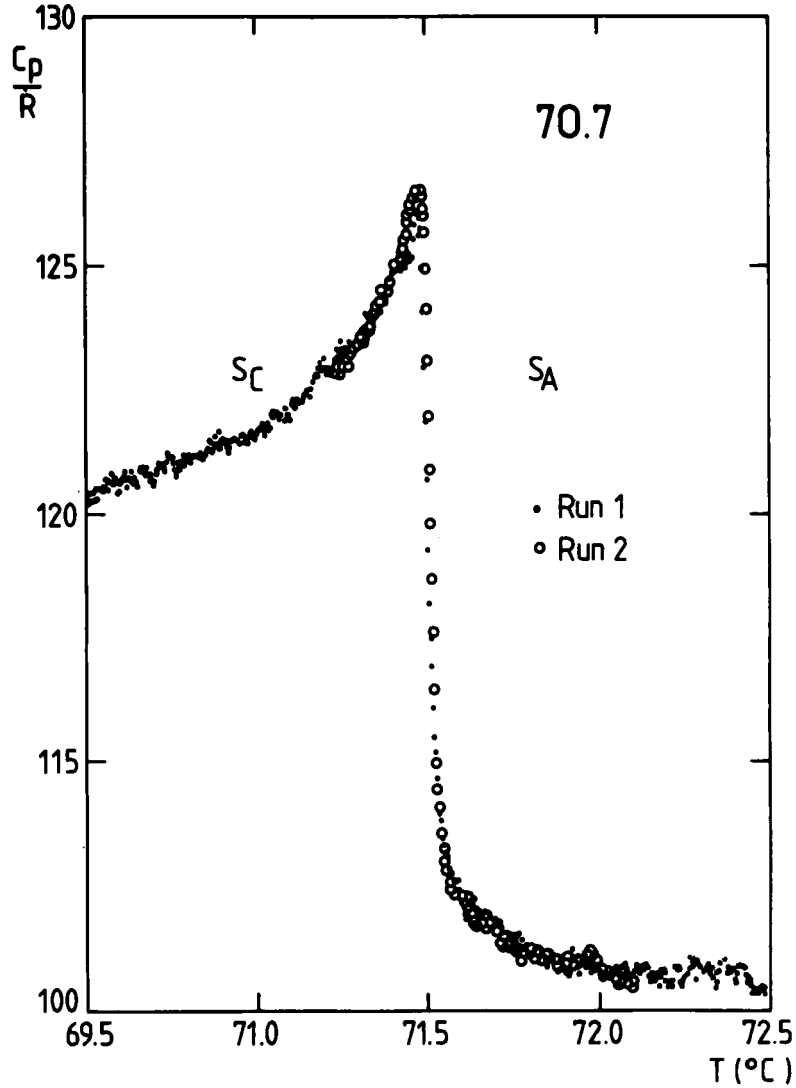


FIGURE 5 Detailed plot of the reduced heat capacity per mole for 70.7 near the smectic C to smectic A phase transition. Data of two different runs (see Table I) have been displayed.

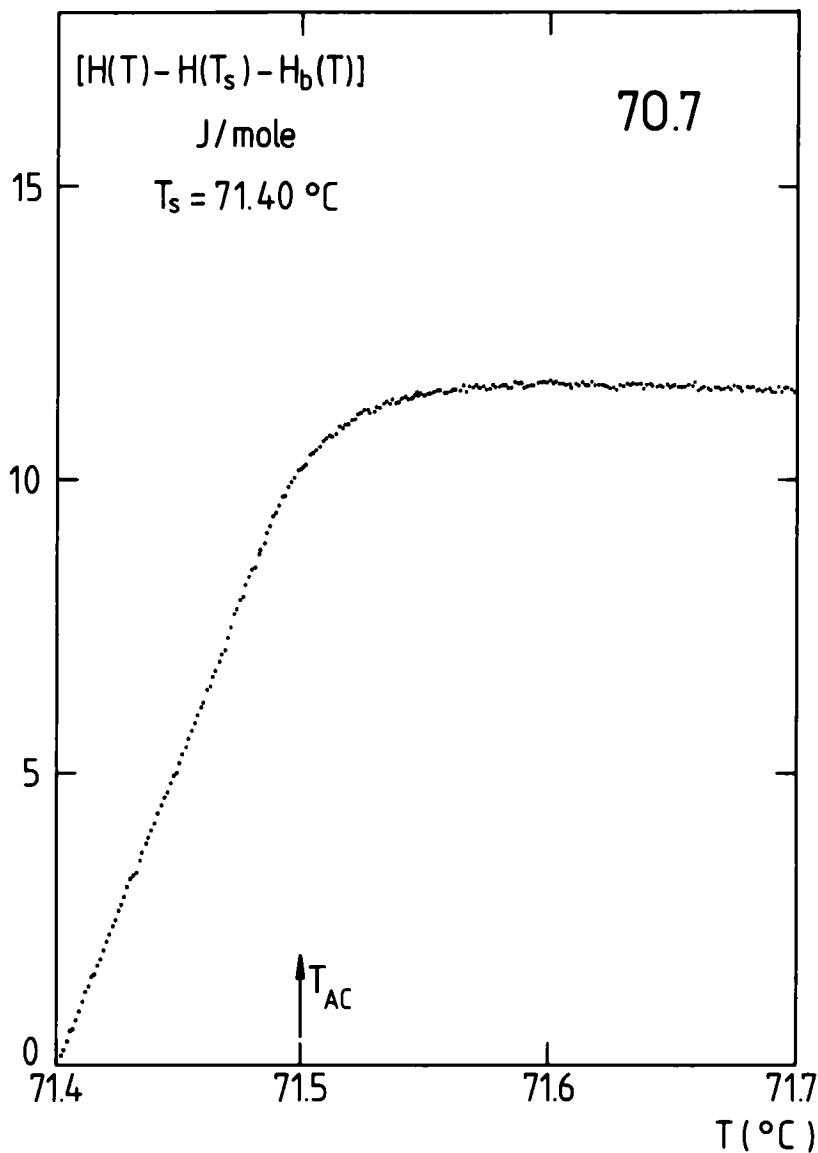


FIGURE 6 Detailed plot of the enthalpy near the AC transition in 7O.7. Note that for clarity a large background  $H_b(T)$  (see text) has been subtracted from the direct data.

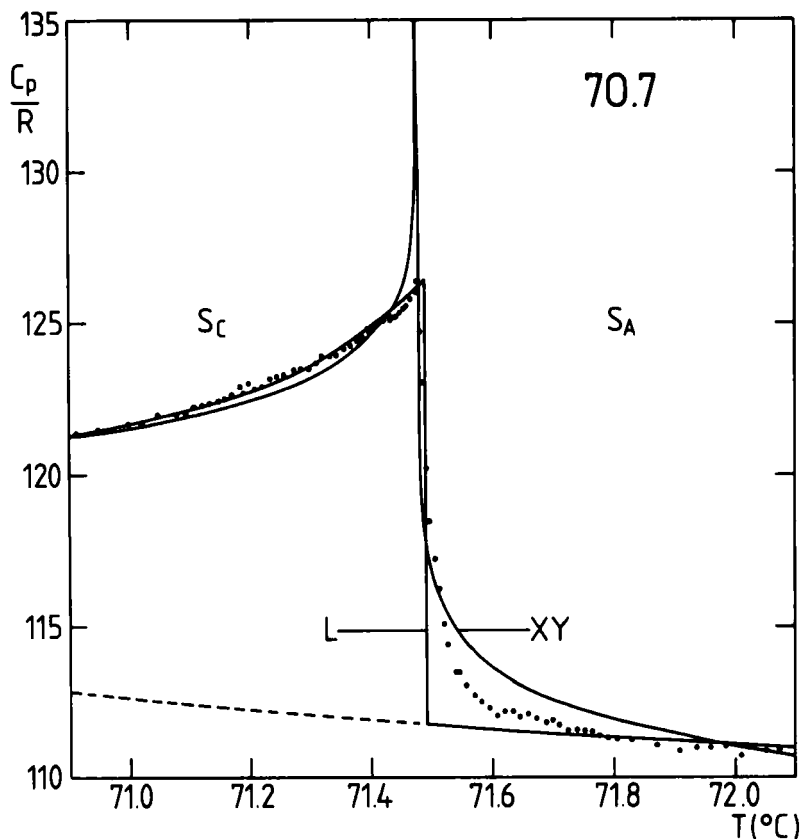


FIGURE 7 Comparison between experimental  $C_p/R$  data close to the AC transition in 70.7 and theoretical fits with the predictions by the XY-model (XY) and the Landau (L) meanfield model with a sixth order term included in the free energy. For the XY-curve parameters of fit XY-2 of Table II and for the L-curve parameters of fit L-8 of Table III have been used.

the data of run 2 we arrive at an upper limit of 1 J/mole for a possible latent heat. In fact, our data for the AC transition in 70.7 indicate a continuous second order phase transition.

Both the smectic A and C phase have a layered structure characterized by a one dimensional density wave which has a wave vector parallel (A phase), or tilted (C phase) with respect to the average orientation (indicated by the director) of the long molecular axis. The C order is characterized by a two component order parameter with an amplitude (the tilt angle) and a phase (the azimuthal tilt direction). On the basis of a simple model de Gennes<sup>1,23</sup> predicted that this transition should be second order and belong to the uni-

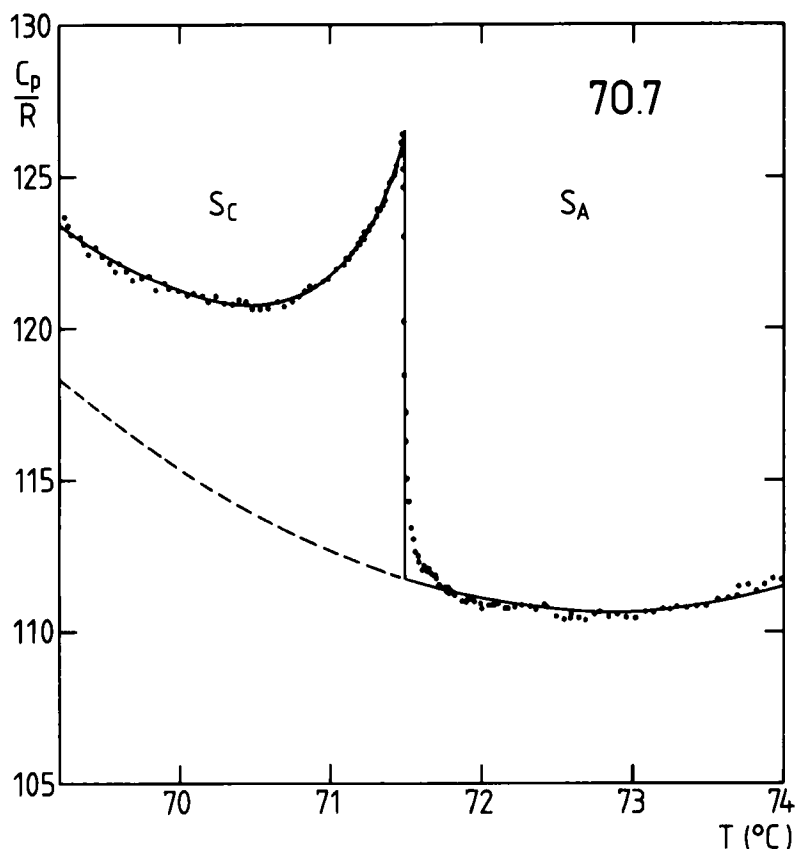


FIGURE 8 Comparison between the experimental  $C_p/R$  data for an extended temperature range in the smectic C and A phases of 70.7, and the Landau fit L-8 of Table III, using Eqs. (6), (7) and (8). Note that for  $T < T_{AC}$  the dashed line represents the background behaviour given by Eq. (8).

versality class of the three dimensional (3d) XY model. More recently Grinstein and Pelcovits<sup>24</sup> have reconsidered the AC transition and included elastic and director fluctuations in their theory. Their results are, however, consistent with the XY classification. As far as the heat capacity is concerned one then has the following predictions:<sup>25,26</sup>

$$C_p/R = A\epsilon^{-\alpha}(1 + D\epsilon^{\Delta} + \dots) + B + E(T - T_c) + \dots \text{ for } T > T_c \quad (3)$$

$$C_p/R = A'|\epsilon|^{-\alpha'}(1 + D'|\epsilon|^{\Delta'} + \dots) + B' + E'(T - T_c) + \dots \text{ for } T < T_c \quad (4)$$

where one has  $\epsilon = (T - T_c)/T_c$ , and expects  $\alpha = \alpha' \simeq -0.02$ ,  $B = B'$ ,  $E = E'$ ,  $A/A' \simeq 1.1$ ,  $D/D' \simeq 1$  and  $\Delta = \Delta' \simeq 0.5$ . The leading contributions to the heat capacity singularity are given by  $A\epsilon^{-\alpha}$  and  $A'|\epsilon|^{-\alpha'}$ , also  $(1 + D\epsilon^\Delta + \dots)$  and  $(1 + D'|\epsilon|^{\Delta'} + \dots)$  represent corrections-to-scaling.<sup>27</sup> The other terms in Eqs. (3) and (4) represent the regular behaviour of the heat capacity.

The prediction that the AC transition should be second order is consistent with our enthalpy results given in Figure 6. In order to test the predicted XY behaviour for the specific heat anomaly we have carried out several curve fits<sup>28</sup> for the  $C_p/R$  data near the AC transition using Eqs. (3) and (4). Since the temperature interval between subsequent data points is about 1 mK it was not feasible to fit all these data directly with the minimization program. Instead we selected 160 data points in the temperature range between 69.2°C and 74°C.

Since only data close to the critical point ( $|\epsilon| < 4 \times 10^{-3}$ ) have been included in testing the XY predictions, it was assumed that correction-to-scaling terms could be neglected. This assumption was, however, also verified by the procedure of range shrinking. In all the curve fits the critical exponents have been given the theoretical value  $\alpha = \alpha' = -0.02$ . Also the critical temperature was given a fixed value in the fitting procedure. The influence of the experimental uncertainty on the critical temperature was investigated by making different choices for  $T_c$ .

The results are summarized in Table II. For each fit  $\chi^2_\nu$ , the reduced chi-square value, is also given as a measure for the fitting quality.<sup>29</sup> In a first series of curve fits (XY-1 to XY-8 in Table II) the data below and above  $T_c$  have been fitted simultaneously for two different ranges of the reduced temperature difference  $\epsilon$ :  $-2.6 \times 10^{-3} \leq \epsilon \leq 3.2 \times 10^{-3}$  and  $-10^{-3} \leq \epsilon \leq 10^{-3}$ . For the curve fits XY-1 to XY-6 we imposed the theoretically expected constraints  $B = B'$  and  $E = E'$ . Under these conditions one obtains very bad fitting with large  $\chi^2_\nu$  values and large systematic deviations. Changes in  $T_c$  or  $\epsilon_{\max}$  and  $\epsilon_{\min}$  do not make very much difference. Relaxing the constraints  $B = B'$  and  $E = E'$  does, however, appreciably improve the curve fits as can be seen in Table II from the smaller  $\chi^2_\nu$  values for the fits XY-7 and XY-8. If the data above and below  $T_c$  are analysed separately (fits XY-9 to XY-12) it appears that the data in the smectic C phase are very well described by Eq. (3), but that the data in the A phase are incompatible with the XY-behaviour included in the form of Eq. (4). The large differences in  $A, A'$ ,  $B, B'$  and  $E, E'$  also lead to the conclusion that the XY-model does not give a useful description of the complete AC critical region. This is further illustrated in Figure 7 where the experimental data are compared with fit XY-2.

TABLE II  
Parameter values from XY-fits to the data above and below the smectic A to C phase transition ( $T_c = T_{AC}$ )  
with Eq. (3) for  $T > T_c$  and the Eq. (4) for  $T < T_c$

Fit	$T_c$ (°C)	$A'$	$A$	$B'$	$B$	$E'$	$E$	$10^3 \epsilon_{\min}$	$10^3 \epsilon_{\max}$	$\chi^2$
XY-1	(71.475) <sup>a</sup>	- 90.6	- 102.3	201.0	( $B'$ )	- 0.16	( $E'$ )	- 2.6	3.2	37.5
XY-2	(71.478)	- 94.7	- 106.7	204.7	( $B'$ )	0.08	( $E'$ )	- 2.6	3.2	31.6
XY-3	(71.481)	- 96.8	- 109.1	206.5	( $B'$ )	0.31	( $E'$ )	- 2.6	3.2	25.8
XY-4	(71.475)	- 107.1	- 116.4	214.0	( $B'$ )	- 7.29	( $E'$ )	- 1.0	1.0	41.3
XY-5	(71.478)	- 113.9	- 123.7	220.0	( $B'$ )	- 6.37	( $E'$ )	- 1.0	1.0	33.4
XY-6	(71.481)	- 116.1	- 126.6	222.1	( $B'$ )	- 5.33	( $E'$ )	- 1.0	1.0	26.1
XY-7	(71.478)	- 44.9	- 225.0	162.7	304.1	2.87	- 7.34	- 2.6	3.2	8.60
XY-8	(71.478)	- 25.5	- 325.0	146.7	386.4	6.27	- 24.9	- 1.0	1.0	3.43
XY-9	(71.478)	- 44.9	—	162.7	—	2.87	—	- 2.6	0.0	1.46
XY-10	(71.478)	- 25.5	—	146.7	—	6.27	—	- 1.0	0.0	0.65
XY-11	(71.478)	—	- 225.0	—	304.1	—	- 7.34	0.0	3.2	16.6
XY-12	(71.478)	—	- 325.0	—	386.4	—	- 24.8	0.0	1.0	7.10

<sup>a</sup> Parameter values between parentheses indicate that the parameter was held constant at the quoted value.

The same incompatibility between the XY predictions and experimental heat capacity data was also recently demonstrated by Meichle and Garland<sup>10</sup> for AMC-11 (azoxy-4,4'-di-undecyl- $\alpha$ -methylcinnamate). In fact all available high-quality calorimetric data of the AC transition lack the characteristic  $\lambda$ -type behaviour predicted by the XY-model, which is experimentally found at the  $\lambda$ -point of helium.

Particularly in the smectic A phase the  $C_p$  behaviour looks qualitatively different: there are almost no pretransition effects and  $C_p$  jumps suddenly at the transition. These features are indicative of a classical meanfield behaviour. The apparently meanfield behaviour of the early<sup>30</sup> heat capacity data for 8S5 and other similar indications from X-ray work were explained by Safinya *et al.*,<sup>31</sup> who used a Landau-Ginzburg model and argued that the bare correlation length characterizing tilt fluctuations is generally quite large so that the true XY critical region should be unobservably small. This was recently<sup>9</sup> confirmed for 4O.7 where, on the basis of calorimetric, X-ray and light scattering experiments, it was shown that the true critical region should only be present for  $\epsilon < 10^{-5}$ . The meanfield model is also supported by recent ac-calorimetric work.<sup>32-35</sup> It was, however, pointed out by Huang and Viner<sup>32</sup> that it is necessary to retain the sixth order term in the Landau free energy expansion in order to arrive at a proper description of the experimental results. Starting with a free energy expression

$$G = G_o + a \epsilon \phi^2 + b \phi^4 + c \phi^6, \quad (5)$$

where  $\phi$  is the tilt order parameter, one arrives at:

$$C_p/R = C_p^o/R \quad \text{for } T > T_c, \quad (6)$$

$$C_p/R = C_p^o/R + A \frac{T}{T_c} \left( \frac{T_m - T_c}{T_m - T} \right)^{1/2} \quad \text{for } T < T_c, \quad (7)$$

where  $A \equiv a^2/2b R T_c$ ,  $T_m \equiv T_c + (b^2 T_c/3ac)$ , and  $C_p^o$  is the background heat capacity arising from the regular part  $G_o$ . For a continuous transition (at  $\epsilon = 0$ ), as observed for the AC transition, one must have  $b \geq 0$  and  $a, c > 0$ . If  $b = 0$  a tricritical point is observed and a diverging  $C_p$  is predicted below  $T_c$  with a critical exponent  $\alpha' = 0.5$ . Above  $T_c$  the heat capacity remains equal to the regular part  $C_p^o$ . If  $b > 0$ , one has an ordinary second order transition that might be quite close to a tricritical point.

We now want to discuss the comparison we have made between



our experimental data and the  $C_p$  behaviour predicted by the Landau model. In our comparison with the XY model we looked for the asymptotic critical behaviour and restricted the analysis to the temperature range of a few tenths of a degree above and below  $T_{AC}$ . In that case a linear temperature dependence for the background in Eqs. (4) and (5) was sufficient. However, if one wants to analyse the data over a wider temperature range a complication arises because of the plastic crystalline B phase (only about 2.3°C below  $T_{AC}$ ). As can be seen in Figure 2 the AC transition seems to be superimposed on a nonlinear precursor increase associated with the BC transition. A similar precursor effect was observed for other compounds of the nO.m series at the transition from a liquid crystalline to a plastic crystalline state.<sup>7,10</sup> The case of 4O.8 is of particular interest because it showed the occurrence of the precursor effect in the smectic A phase above the AB transition temperature without the interference of an AC transition. This effect, which was observable for 2–3°C above the AB transition, was ascribed to growing short-range order in the smectic layers.<sup>7</sup> This effect seems to occur for the smectic C as well as for the smectic A layered structure. In order to account for this effect we have introduced higher order terms in the expression for the  $C_p$  behaviour in the A and the C phase:

$$C_p/R = B + E(T - T_c) + F(T - T_c)^2 + \dots \quad (8)$$

The parameter values for fits to our 7O.7 data with Eqs. (6), (7) and (8) are summarized in Table III. The fits have been carried out for the temperature range between 69.2°C (the BC transition) and 74°C. From Eq. (7) it can be seen that  $C_p$  is expected to make a discontinuous jump  $\Delta C_p$  at  $T_c$  between  $C_p^\infty(T_c)$  and  $C_p^\infty(T_c) + A$ . One can thus expect that for  $T > T_c$  the small pretransitional increase observed close to the transition temperature (see Figures (5) and (6)) will not be described very well by Eq. (8). For this reason data in the temperature interval between  $T_c$  and a chosen temperature  $T_e$  have not been used in the curve fits. However, different choices have been made for  $T_e$  (see Table III). For each choice of  $T_e$  different  $T_c$  values have also been imposed in the fitting procedure. For a given  $T_e$  value the different choices for  $T_c$  have little influence on the quality of the fits. Decreasing  $T_e - T_c$  also does not change markedly the parameter values but gives significantly increased  $\chi^2_\nu$  values. This is a manifestation of the small systematic deviations in the temperature interval between  $T_e$  and  $T_c$ . In all cases, however, the overall quality of the fits remains quite good. This is illustrated in Figure 8 where we used

TABLE III

Parameter values from Landau-fits to the data above and below the smectic A to C phase transition ( $T_c = T_{AC}$ ) with Eqs. (6), (7) and (8). Data between 69.2°C and 74°C have been used in the curve fits, except for the data between  $T_c$  and  $T_c$  which have been excluded from the fits (see text).

Fit	$T_c$	$T_c$	$T_m$	A	B	E	F	$\chi^2$
L-1	(71.52) <sup>a</sup>	(71.48)	71.765	14.2	112.0	-1.66	0.54	3.79
L-2	(71.52)	(71.49)	71.765	14.5	112.0	-1.65	0.54	3.79
L-3	(71.52)	(71.50)	71.765	14.7	112.0	-1.65	0.54	3.79
L-4	(71.55)	(71.48)	71.781	14.4	111.9	-1.59	0.57	1.63
L-5	(71.55)	(71.49)	71.781	14.6	111.8	-1.58	0.57	1.63
L-6	(71.55)	(71.50)	71.781	14.9	111.8	-1.57	0.57	1.63
L-7	(71.60)	(71.48)	71.788	14.4	111.8	-1.57	0.58	1.27
L-8	(71.60)	(71.49)	71.788	14.7	111.8	-1.56	0.58	1.27
L-9	(71.60)	(71.50)	71.788	14.9	111.7	-1.55	0.58	1.27
L-10	(71.70)	(71.48)	71.799	14.5	111.6	-1.53	0.61	0.90
L-11	(71.70)	(71.49)	71.799	14.8	111.6	-1.51	0.61	0.90
L-12	(71.70)	(71.50)	71.799	15.0	111.6	-1.50	0.61	0.90

<sup>a</sup> Parameter values between parentheses indicate that the parameter was held constant at the quoted value.

the parameter values of fit L-8 in Table III. A detailed comparison for a smaller temperature range near  $T_{AC}$  is also given in Figure 7. From both these figures and the results of Table III one can conclude that, with the exception of a small  $\approx 0.2^\circ\text{C}$  wide temperature immediately above  $T_{AC}$ , the Landau expressions give a very good overall description of the heat capacity anomaly near the AC transition in 7O.7. The small pretransitional increase in the smectic A phase may be an indication of the crossover to the experimentally not accessible XY critical region. Although there are no correlation length data available for 7O.7, to allow estimation of the critical region, the analysis of our  $C_p$  results shows that it must be very small.

In comparing AC-transitions in different materials one often uses an important parameter  $\epsilon_o$ , introduced by Huang and Viner<sup>32</sup> to characterize the shape of the excess heat capacity. This parameter  $\epsilon_o$  is related to the coefficients in Eq. (5) by:

$$\epsilon_o \equiv 3(T_m - T_c)/T_c = b^2/ac. \quad (9)$$

It characterizes the full width at half height ( $A/2$ ) of the meanfield heat capacity anomaly. From the results of Table III we arrive at a value  $\epsilon_o = (2.8 \pm 0.2) \times 10^{-3}$ . This value is about 2 to 3 times larger than for the other members of the nO.m series, which have previously been investigated:<sup>10</sup>  $\epsilon_o = 1.6 \times 10^{-3}$  for 7O.6,  $\epsilon_o = 1.3 \times 10^{-3}$  for 4O.7 and  $\epsilon_o = 0.8$  for 7O.4. Our value is, however, 2 to 3 times smaller than  $\epsilon_o$  values for some other liquid crystals<sup>10</sup> not belonging to the nO.m series. A small  $\epsilon_o$  value could indicate the closeness of a classical tricritical point ( $b = 0$ ).<sup>36</sup>

The possibility of an AC tricritical point was very recently reconsidered by Lien and Huang.<sup>37</sup> They observed that, if they left out the compounds with a nematic range, a possibly general relation emerged between  $\epsilon_o$  and  $T_{AC}/T_{IA}$  for compounds with an I-A-C (or C\*: chiral C) transition sequence. Although 7O.7, strictly speaking, does not have the required sequence, it certainly is a borderline case because it only has a  $0.3^\circ\text{C}$  wide nematic range between the  $12^\circ\text{C}$  wide A phase and the isotropic phase. If we neglect this N range, our  $\epsilon_o (= 2.8 \pm 0.2 \times 10^{-3})$  value for  $T_{AC}/T_{IA} = 0.965$  (with the very good approximation that  $T_{IA} = T_{NI}$ ) fits in reasonably well with the nearly linear behaviour observed by Lien and Huang for systems with small  $T_{AC}/T_{IA}$ . The fact that  $\epsilon_o$  seems to go to zero with  $T_{AC}/T_{IA}$ , does not necessarily imply that  $b$  approaches zero, because the parameter  $c$  and/or  $a$  in Eq. (5) can become abnormally large with  $b$  remaining finite such that  $\epsilon_o$  apparently approaches zero. If, however, tilt angle

data are also available it is possible to calculate the coefficients  $a$ ,  $b$  and  $c$  in Eq. (5) separately. This was done by Lien and Huang<sup>37</sup> for four compounds with the I-A-C sequence. For three of the compounds all the coefficients monotonically decrease as  $T_{AC}/T_{IA}$  increases. For the fourth material MBRA8 (S-4-O-(2-methyl) butylresorcyldiene-4'-octylaniline) with the smallest  $\epsilon_o$  ( $= 0.9 \times 10^{-3}$ ) value quite large  $a$ ,  $b$  and  $c$  values were determined. In particular  $c$  was unusually large, resulting in the observed small  $\epsilon_o$ . Thus, apparently at the moment there is no unambiguous evidence for the existence of an AC tricritical point. So far all high resolution data indicate second order AC transitions.

### 3. The BC transition

The liquid crystalline B phase is characterized by hexagonal order within each layer. It has, however, recently become clear that for several compounds many of the phases previously classified as smectic B phases are not genuine liquid crystal phases but plastic crystalline phases. Indeed two possible classes seem to exist: a plastic crystalline B phase with long range three dimensional positional order and an hexatic B phase with long range bond orientational order but with short range positional order in the layers.<sup>3-6,11,38-40</sup> In the case of 7O.7 it was shown from X-ray investigations that the B phase (and also the G phase below it) is not a liquid crystal phase but a plastic B phase with weak interlayer coupling.<sup>3,4,40</sup>

In the smectic C phase the molecules are tilted with respect to the layer normal, but in the B phase the director and the layer normal are again parallel. Therefore, unless there is a pretransitional return to zero tilt in the C phase, one should expect a first order smectic C to plastic B transition. As can be seen in Figure 9 from the enthalpy behaviour this transition is indeed strongly first order. The latent heat for this transition is  $2.9 \pm 0.1$  kJ/mole. There is also a rather broad two-phase region between 68.69°C and 69.21°C. The temperature dependence of  $C_p/R$  near this transition can be observed in Figure 2. There is no significant pretransitional increase in the B phase on approaching the transition. This is in contrast to an effect observed in the B phase of 4O.8 near the BA transition.<sup>7</sup> In that case the effect was associated with changes in the defect structure prior to melting. If these changes also occur for 7O.7 on approaching the BC transition, it turns out that the  $C_p$  behaviour is less affected. The pretransitional effect in the C phase has already been considered in Sec. 2, and is similar to that observed for other compounds of the nO.m series.<sup>7,10</sup>

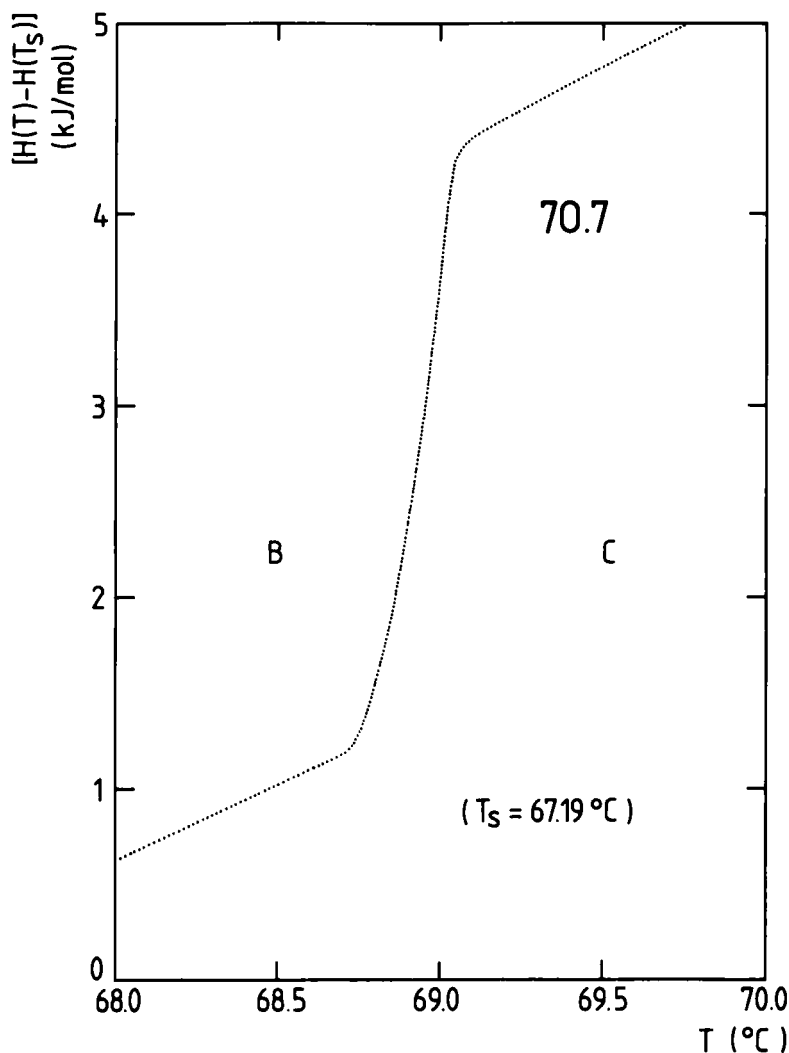


FIGURE 9 Temperature dependence of the enthalpy near the B or C transition in 7O.7.

#### 4. The restacking transitions in the B phase

In a recent high-resolution X-ray diffraction study of freely suspended films of 7O.7 Collett *et al.*<sup>12</sup> observed several restacking transitions in the B phase. Because the interlayer coupling is much smaller than the intralayer coupling, layers can easily shift relative positions of adjacent layers, giving rise to different crystalline structures. The

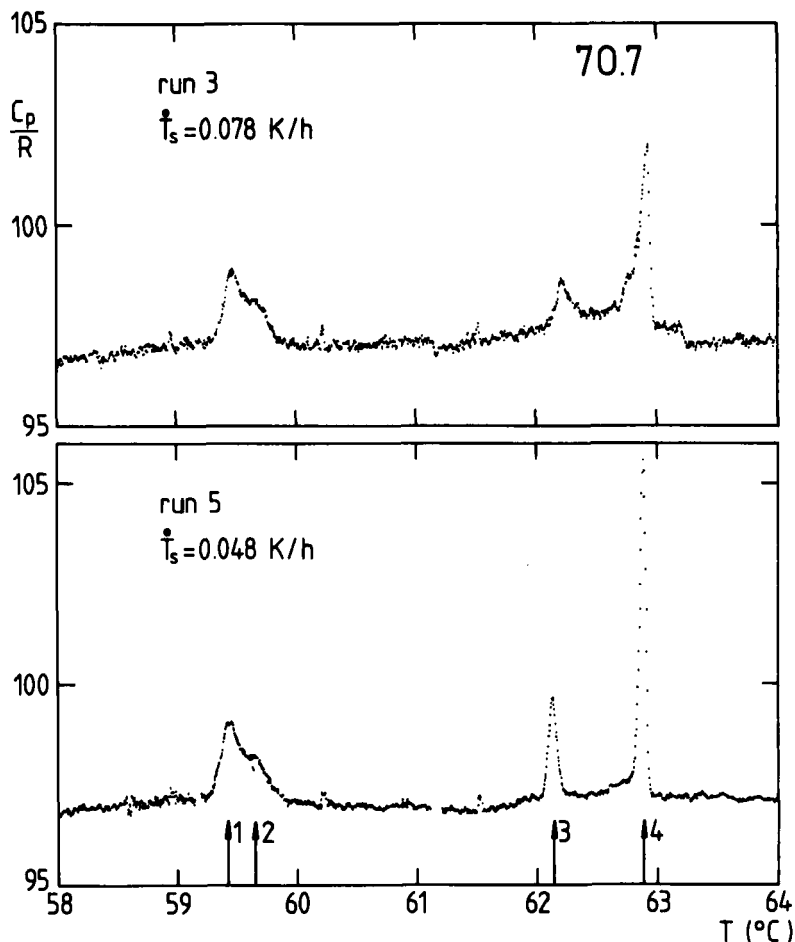


FIGURE 10 The reduced heat capacity per mole in the B phase of 70.7, showing several thermal anomalies.

detailed nature of these subtle transitions has been considered a mystery because no latent heat or other thermal anomaly could be detected.<sup>12</sup>

We have carried out a detailed high-resolution thermal investigation of the entire B phase of 70.7. From this study it turned out that several thermal anomalies could be observed. Three runs (run 3 to 5 in Table I) have been carried out in the B phase. Run 3 spans the entire B phase, run 4 gives the GB transition and part of the B phase up to 57.3°C, while run 5 covers the most interesting part of the B phase between 57.9°C and 64.6°C. Figure 10 gives the  $C_p/R$  behaviour

as observed in run 3 and 5 for the temperature range between 58°C and 64°C. For the B phase outside this range no thermal features have been measured (see also Figures 2 and 12). As can be seen from Figure 10 both runs are in quite good agreement. The resolution of run 5 is, however, somewhat better because a lower scanning rate (0.048 K/h versus 0.078 K/h) has been used. The same anomalies appear in both sets of data. Between 59°C and 60°C a broad double peaked anomaly appears. In addition to that, two distinct  $C_p$  peaks are present at about 62.1°C and 62.9°C. It should be noted that although the anomalies are clearly visible, the  $C_p/R$  increases are only of the order of 2% for the lowest three peaks and less than 10% for the fourth.

Table IV gives a possible correspondence between the temperatures of the restacking transitions, as observed in the X-ray study,<sup>12</sup> and the heat capacity peak temperatures. If we allow for a small systematic temperature difference of about 0.2°C (which could easily come from different impurity concentrations in the samples) between the X-ray work and our calorimetric results, there seems to be a rather close coincidence between the peaks 1, 2, 4 and the three different restacking transitions reported. Thus, contrary to previous reports,<sup>12</sup> there seem to be thermal anomalies associated with these transitions. There remains, however, a problem because our peak 3 at 62.1°C does not correspond to any feature in the X-ray work so far reported. As an additional verification for the anomalies shown in Figure 10, we carried out a quick test run about 6 months later and after the sample was heated (in the sample cell) to the isotropic phase and well stirred. All four anomalies were observed again at nearly the same temperatures.

TABLE IV

Possible correspondence between the restacking transitions observed in an X-ray diffraction study (Ref. 12) and the heat capacity peaks in the smectic B phase of 70.7.

structure (from X-ray)	$T$ of the transitions (from X-ray)	$T$ of the $C_p$ peaks
hexagonal AAA	59.75°C	59.41°C
monoclinic C	60.1°C	59.64°C
orthorhombic F		62.12°C
	63.0°C	62.88°C
hexagonal ABAB		

Because of the smallness of the anomalies it was quite difficult to determine the order of the phase transitions involved. This was certainly the case for the first two peaks because there was a rather smooth  $T$  dependence of the enthalpy for the entire width of the two peaks. On the basis of small jumps in the adjacent layer spacing, it was concluded by Collett *et al.*<sup>12</sup> that the corresponding restacking transitions (see Table IV) were first order. If we interpret  $\int \Delta C_p(T) dT$  (with  $\Delta C_p(T) = C_p(T) - 97 R$ ) between 59.25°C and 59.90°C (the entire width of the two peaks) as latent heat we arrive at 20 J/mole for both transitions together. Also the restacking transition (at  $T = 63^\circ\text{C}$ ) from orthorhombic F to hexagonal ABAB, corresponding with our peak 4, showed an abrupt first order jump in the layer spacing.<sup>12</sup> This is in accordance with the results of run 5 because of the sharpness of the peak and the sudden changes in the temperature dependence of  $C_p/R$ . The same arguments seem to hold for peak 3. The temperature dependence of the enthalpy for both transitions is displayed in Figure 11. For display reasons a large linear part  $97 R(T - T_0)$  has again been subtracted from the direct  $H(T)$  data. As an estimate for the latent heats for these transitions we arrive at  $\Delta H = (5 \pm 2)$  J/mole for peak 3 and at  $\Delta H = (10 \pm 2)$  J/mole for peak 4.

### 5. The G to B transition

Collett *et al.*<sup>12</sup> and also previously Goodby *et al.*<sup>6</sup> observed, in the B phase of 7O.7, a small one-dimensional modulation (in the direction perpendicular to the layers) of the density wave characterizing the layered structure. This modulation has a periodicity of about 20 molecular lengths. The effect is believed to originate from a sinusoidal tilt deformation. The amplitude of the modulation increased with decreasing temperature and it was suggested<sup>3,6</sup> that this effect eventually triggers the transition from the smectic A like plastic B phase to the smectic C like plastic G phase.

On the basis of X-ray work, Doucet and Levelut<sup>40</sup> came to the conclusion that the GB transition in 7O.7 was first order. Although no data very close to  $T_{GB}$  were obtained ( $T_{GB} - T > 1^\circ\text{C}$ ), the tilt angle appeared to make a  $20^\circ$  jump at the transition.

We have carried out three different runs through the G to B transition (runs 4, 8 and 9). The  $C_p/R$  results of the heating run 4 are displayed as part of Figure 2. The cooling run 8 and a second heating run 9 have been carried out about 6 months after run 4.  $C_p/R$  results for those two runs are given in Figure 12. Apart from a small 0.07 K decrease in  $T$  of the  $C_p/R$  maximum of run 9, there are no important



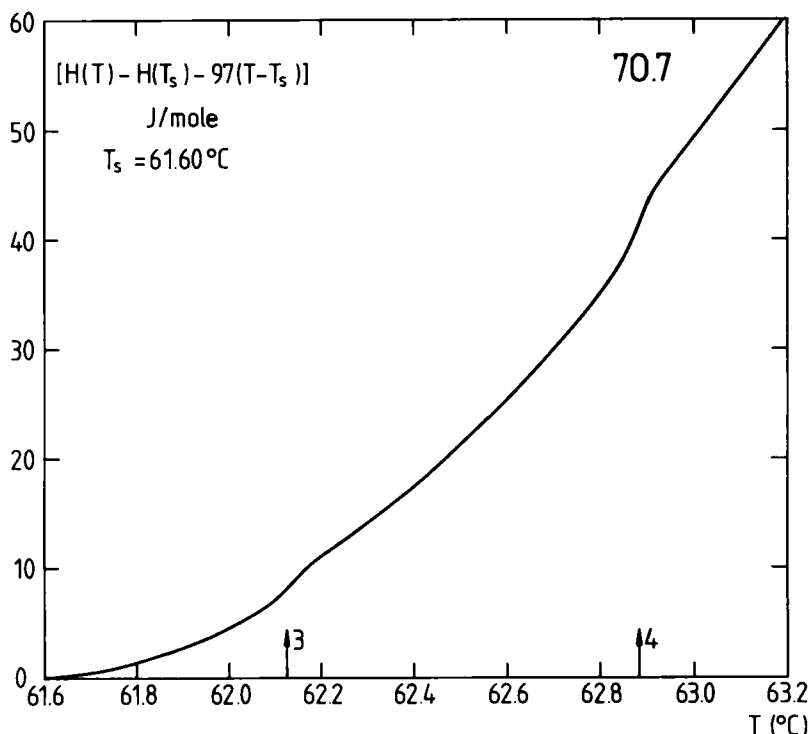


FIGURE 11 Detailed plot of the enthalpy for the temperature range of two  $C_p/R$  peaks in Figure 10. Note that for clarity a large linear background  $C_p^\infty (T - T_s)$ , with  $C_p^\infty = 97 R$ , has been subtracted from the raw data.

differences between the two heating runs. Both runs show a sharp rise on the G side of the transition and a gradual decrease over nearly  $1^\circ\text{C}$  in the B phase. A completely opposite picture is given by the cooling run 8. In that case there is a sharp rise on the B side of the transition and a gradual decrease in the G phase also over nearly a  $1^\circ\text{C}$  wide temperature range. The sharp breaks in  $C_p/R$  at the transition in the G phase on heating and in the B phase on cooling are indicative of a first order character for the transition. The temperature of the  $C_p/R$  maxima for the cooling and the heating run are almost identical and are consistent with  $T_{GB} = 53.7 \pm 0.1^\circ\text{C}$ . It is, however, also clear that the latent heat of the transition is smeared out over about  $1^\circ\text{C}$  in the B phase on heating and in the G phase on cooling. This hysteresis effect can also be clearly observed in the enthalpy behaviour of run 8 and 9 given in Figure 13. Although our scanning rates are very slow ( $\dot{T} \approx 0.05 \text{ K/h}$ ) full thermodynamic equilibrium

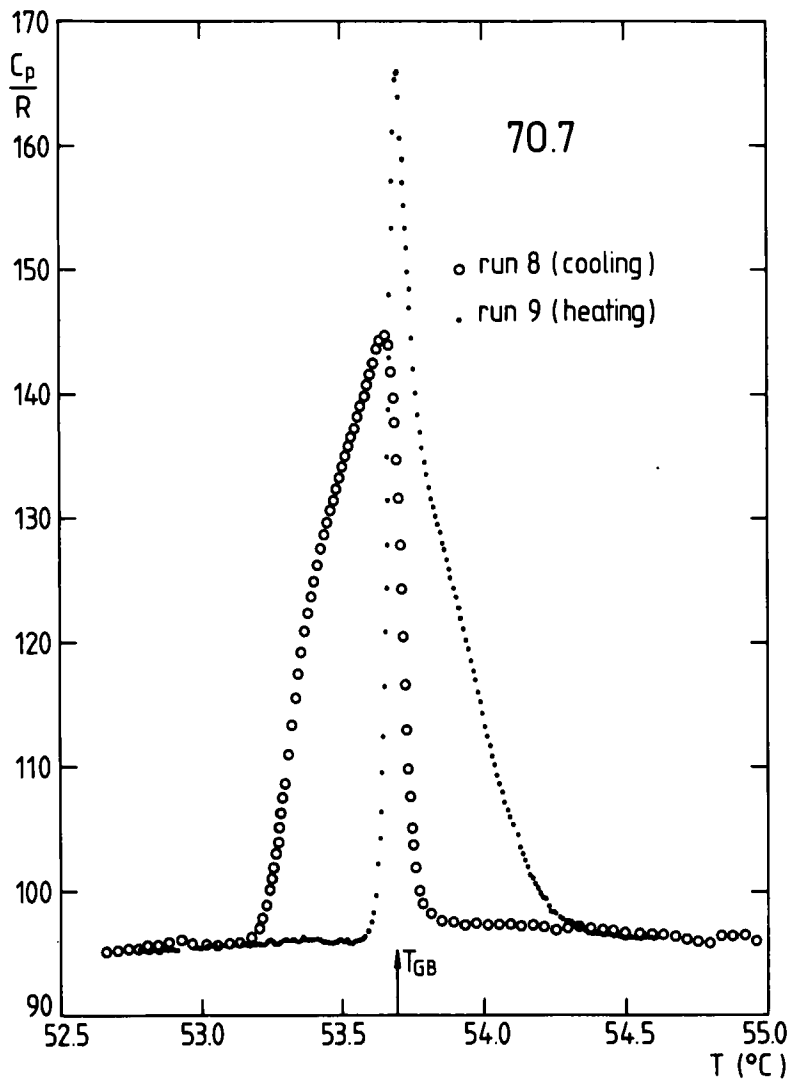


FIGURE 12 Detailed plot of the reduced heat capacity per mole for a heating and a cooling run through the G to B transition in 70.7.

is apparently not reached in that  $1^{\circ}\text{C}$  wide  $T$ -range after entering the new phase.

A value for the latent heat can be obtained from

$$\int_{T_1}^{T_2} (C_p - C_p^{\infty}) dT = H(T_2) - H(T_1) - \int_{T_1}^{T_2} C_p^{\infty} dT, \quad (10)$$

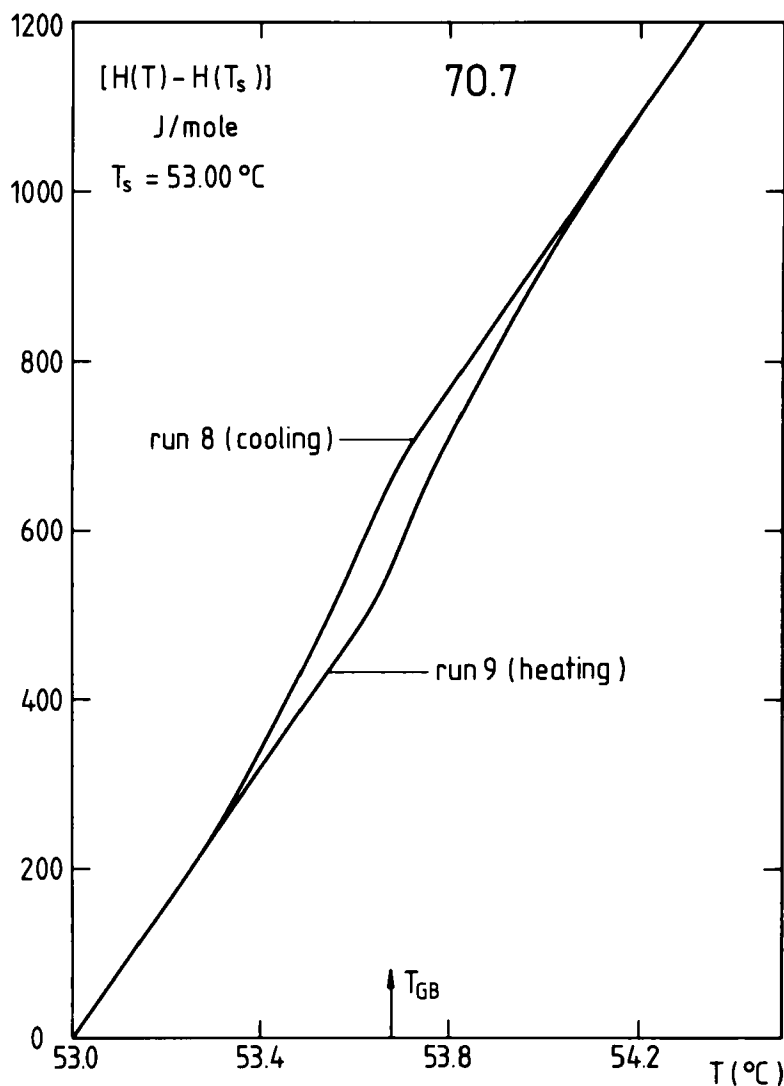


FIGURE 13 The temperature dependence of the enthalpy from a heating and a cooling run through the G to B transition in 70.7.

where  $C_p^\infty$  is the background behaviour of the heat capacity and where  $T_2 - T_1$  is the entire width of the  $C_p$  peaks for the GB transition in Figures 12 and 2. If we apply Eq. (10) to the results of our three runs for the GB transition (runs 4, 8 and 9 in Table I), we arrive at a value  $\Delta H_L = 0.135 \pm 0.015$  kJ/mole for the latent heat. The uncertainty

in  $\Delta H_L$  arises mainly from uncertainties in the  $C_p/R$  choices ( $96.5 \pm 1.0$ ). From DSC measurements Doucet and Levelut<sup>40</sup> estimated  $\Delta H_L < 0.4$  kJ/mole which is consistent with our result.

## SUMMARY AND CONCLUSIONS

In this paper we have presented new experimental data for the temperature dependence of the enthalpy and the heat capacity of the liquid crystalline material heptyloxybenzylidene-heptylaniline (7O.7). The rich variety of phases and phase transitions occurring in the temperature range between 52°C and 86°C has been studied in detail. As pointed out in the experimental section our measuring procedure allows us to obtain results for the heat capacity as well as for the enthalpy including latent heats if present.

Although the transition temperatures for the isotropic to nematic (NI) and nematic to smectic A (NA) transitions differ only 0.3°C, the two transitions could be well separated by our calorimetric method. The NI as well as the NA transitions are both first order with a latent heat of  $2.1 (\pm 0.1)$  kJ/mole and  $(2.2 \pm 0.1)$  kJ/mole respectively. The first order nature of the NA transition is in agreement with recent observations for systems with similarly small nematic ranges.<sup>16,22</sup>

The phase transition between the smectic A and the smectic C (AC) phases is, within our experimental resolution, a purely continuous second order transition. As an upper limit for the latent heat, we arrive at a value of 1 J/mole. The heat capacity anomaly at this AC transition is not consistent with the theoretically predicted XY behaviour. It can, however, be described rather well with meanfield expressions derived from a Landau free energy expansion including a sixth order term. This is in agreement with the conclusions for AC transitions in other systems.<sup>9,10,32-35</sup> In the case of 4O.7, another compound of the same nO.m homologous series as 7O.7, this meanfield behaviour can be explained<sup>9</sup> in terms of the Ginzburg criterion, which shows that the XY critical behaviour in 4O.7 occurs for reduced temperatures less than  $10^{-5}$ . Apparently the same conclusion should be reached for 7O.7.

The transition from the smectic C to the plastic crystalline B phase is first order with a large latent heat of  $2.9 (\pm 0.1)$  kJ/mole. The transition between the plastic B and G phases is also first order, but with a rather small latent heat of  $0.135 (\pm 0.015)$  kJ/mole.

In a recent high-resolution X-ray diffraction study of freely suspended films of 7O.7 Collett *et al.*<sup>12</sup> observed three restacking tran-

sitions in the B phase between 55°C and 69°C. Previously no latent heats or other thermal anomaly could be associated with these transitions.<sup>12,40</sup> From our detailed study it turned out that four thermal anomalies could be clearly observed. For three of these a possible correspondence with the restacking transitions, observed by Collett *et al.*,<sup>12</sup> could be established. One thermal anomaly (at 62.1°C), however, does not correspond to any feature of the X-ray work reported so far.

## References

1. P. G. de Gennes, *The Physics of Liquid Crystals* (Clarendon, Oxford, 1974).
2. G. W. Smith and Z. G. Garlund, *J. Chem. Phys.*, **59**, 3214 (1973).
3. A. J. Leadbetter, M. A. Mazid, B. A. Kelly, J. W. Goodby and G. W. Gray, *Phys. Rev. Lett.*, **43**, 630 (1979).
4. A. J. Leadbetter, J. C. Frost and M. A. Mazid, *J. Phys. Lett. (Paris)*, **40**, L-325 (1979).
5. J. W. Goodby, G. W. Gray, A. J. Leadbetter and M. A. Mazid, *J. Phys. (Paris)*, **41**, 591 (1980).
6. J. W. Goodby, G. W. Gray, A. J. Leadbetter and M. A. Mazid in *Liquid Crystals of One- and Two-Dimensional Order* (Eds. W. Helfrich and G. Heppke, Springer, Berlin, 1980) pp. 3–18.
7. K. J. Lushington, G. B. Kasting and C. W. Garland, *J. Phys. Lett. (Paris)*, **41**, L-419 (1980).
8. E. Bloemen and C. W. Garland, *J. Phys. (Paris)*, **42**, 1299 (1981).
9. R. J. Birgeneau, C. W. Garland, A. R. Kortan, J. D. Litster, M. Meichle, B. M. Ocko, C. Rosenblatt, L. J. Yu and J. Goodby, *Phys. Rev. A.*, **27**, 1251 (1983).
10. M. Meichle and C. W. Garland, *Phys. Rev. A.*, **27**, 2624 (1983).
11. D. E. Moncton and R. Pindak, *Phys. Rev. Lett.*, **43**, 701 (1979).
12. J. Collett, L. B. Sorensen, P. S. Pershan, J. D. Litster, R. J. Birgeneau and J. Als-Nielsen, *Phys. Rev. Lett.*, **49**, 553 (1982).
13. B. M. Ocko, A. R. Kortan, R. J. Birgeneau and J. W. Goodby, *J. Phys. (Paris)*, **45**, 113 (1984).
14. J. Thoen, H. Marynissen and W. Van Dael, *Phys. Rev. A.*, **26**, 2886 (1982).
15. H. Marynissen, J. Thoen and W. Van Dael, *Mol. Cryst. Liq. Cryst.*, **97**, 149 (1983).
16. J. Thoen, H. Marynissen and W. Van Dael, *Phys. Rev. Lett.*, **52**, 204 (1984).
17. J. Thoen, E. Bloemen, H. Marynissen and W. Van Dael, *Proceedings of the 8th Symposium of Thermophysical Properties*, Natl. Bur. Stand., Maryland, 1981 (American Society of Mechanical Engineers, New York, 1982).
18. G. B. Kasting, K. J. Lushington and C. W. Garland, *Phys. Rev. B.*, **22**, 321 (1980).
19. We thank Professors C. W. Garland and J. D. Litster for making the material available to us.
20. P. G. de Gennes, *Solid State Commun.*, **10**, 753 (1972).
21. W. L. McMillan, *Phys. Rev. A.*, **4**, 1238 (1971).
22. B. M. Ocko, R. J. Birgeneau, J. D. Litster and M. E. Neubert, *Phys. Rev. Lett.*, **52**, 208 (1984).
23. P. G. de Gennes, *Mol. Cryst. Liq. Cryst.*, **21**, 49 (1973).
24. G. Grinstein and R. A. Pelcovits, *Phys. Rev. A.*, **26**, 2196 (1982).
25. J. C. Le Guillou and J. Zinn-Justin, *Phys. Rev. B.*, **21**, 3976 (1980).

26. K. H. Mueller, G. Ahlers and F. Pobell, *Phys. Rev. B.*, **14**, 2096 (1976); G. Ahlers, *Phys. Rev. A.*, **8**, 530 (1973).
27. F. J. Wegner, *Phys. Rev. B.*, **5**, 4529 (1972).
28. We used the CERN computer program MINUIT, CERN computer center program library No. 506.
29. P. R. Bevington, *Data reduction and error analysis for the physical sciences* (McGraw-Hill, New York, 1969).
30. C. A. Schantz and D. L. Johnson, *Phys. Rev. A.*, **17**, 1504 (1978).
31. C. R. Safinya, M. Kaplan, J. Als-Nielsen, R. J. Birgeneau, D. Davidov, J. D. Litster, D. L. Johnson and M. Neubert, *Phys. Rev. B.*, **21**, 4149 (1980).
32. C. C. Huang and J. M. Viner, *Phys. Rev. A.*, **25**, 3385 (1982).
33. C. C. Huang and S. C. Lien, *Phys. Rev. Lett.*, **47**, 1917 (1981).
34. S. C. Lien, J. M. Viner, C. C. Huang and N. A. Clark, *Mol. Cryst. Liq. Cryst.*, **100**, 145 (1983).
35. S. C. Lien, C. C. Huang and J. W. Goodby, *Phys. Res. A.*, **29**, 1371 (1984).
36. C. C. Huang, *Solid State Commun.*, **43**, 883 (1982).
37. S. C. Lien and C. C. Huang, *Phys. Rev. A.*, **30**, 624 (1984).
38. R. J. Birgeneau and J. D. Litster, *J. Phys. Lett. (Paris)*, **39**, L-399 (1978).
39. R. Pindak, D. C. Moncton, S. C. Davey and J. W. Goodby, *Phys. Rev. Lett.*, **46**, 1135 (1981).
40. J. Doucet and A. M. Levelut, *J. Phys. (Paris)*, **38**, 1163 (1977).